Thin Solid Films 545 (2013) 580–583

Contents lists available at ScienceDirect

Thin Solid Films

journal homepage: www.elsevier.com/locate/tsf

Light emission from the Au/CaF_2/p-Si(111) capacitors: Evidence for an elastic electron tunneling through a thin (1–2 nm) fluoride layer

Yu.Yu. Illarionov [a,b,c,*], M.I. Vexler [b], V.V. Fedorov [b], S.M. Suturin [b], N.S. Sokolov [b]

[a] Singapore Institute of Manufacturing Technology, 638075 Nanyang Drive 71, Singapore
[b] Ioffe Physical–Technical Institute, 194021 Polytechnicheskaya 26, St. Petersburg, Russia
[c] Institute for Microelectronics, TU Vienna, 27-29 Gusshausstr., 1040 Vienna, Austria

ARTICLE INFO

Article history:
Received 3 October 2012
Received in revised form 1 July 2013
Accepted 18 July 2013
Available online 24 July 2013

Keywords:
Thin films
Calcium fluoride
Tunnel metal-insulator-silicon structure
Photon emission
Hot electron injection
Molecular beam epitaxy

ABSTRACT

Photon emission from the grown Au/CaF_2/p-Si(111) structures is revealed under the positive substrate bias. This phenomenon occurs due to radiative transitions involving hot electrons injected into silicon. Behavior of light intensity within the selected spectral intervals gives evidence for an elastic tunneling transport through the ultra-thin dielectric film. The result is important considering a perspective of using the epitaxial fluorides as barrier layers in resonant tunneling diodes. Some data of electrical characterization are also included.

© 2013 Elsevier B.V. All rights reserved.

1. Introduction

Calcium fluoride (CaF_2) is a wide-bandgap (12.1 eV) high-permittivity ($\varepsilon = 8.43$) insulator material. Recently, considerable progress has been achieved in understanding growth processes and electrophysical properties of pseudomorphic CaF_2 layers [1,2] grown by molecular beam epitaxy (MBE). Ultra-thin fluoride films are now considered as promising candidates for barrier layers in Resonant-Tunneling Diodes (RTDs) and super-lattices employing Si [3], CdF_2 [4] or Fe_3Si [5] quantum wells. The earlier attempts to fabricate such devices were not unsuccessful [3–5]. They can, at least potentially, exhibit higher peak-to-valley current ratio than the conventional $A^{III}B^{V}$-compound based systems. Furthermore, the Fe_3Si/CaF_2 RTDs may serve as spin injectors.

Despite the undeniable progress in a fluoride film growth, it would be false to claim that the overall technology level in this branch already meets the modern microelectronics standards. So far the quality of the MBE-grown CaF_2 layers is in certain respects inferior to that of the silicon dioxide and some other oxide films. There are also reproducibility problems. For this reason, a reliable diagnostics of thin fluorides in each individual case becomes a primary-importance task. Different measurement techniques can be applied depending on which aspect is focused upon. For example the capacitance-voltage studies would be suitable for studying the CaF_2/Si interface defects. However, in sight of the abovementioned potential applications, it is essential that the barriers de-facto enable an elastic tunnel injection of electrons.

The electron transport can be investigated through mathematical models for any bias condition in simple metal–insulator–semiconductor (MIS) capacitor structures [6,7]. Current–voltage (I–V) characteristics deduced from these models can be compared to the measured data, so that some information on an electron transport within a barrier is recovered. For the perfectly-parameterized systems, like SiO_2/Si, this approach leads to satisfactory results. However, for materials with a rather modest history of study, CaF_2 in this case, a degree of reliability becomes lower due to uncertainty in choosing carrier effective masses, band offsets and also due to consideration of film thickness fluctuations. In other words, a "satisfactory" agreement to experiment can be attained using some doubtful combinations of fitting parameters, thereby masking the real transport picture. For this reason, in the present work, not abandoning the pure-electrical characterization (apropos, the barrier parameters for fluoride are, in principle, known [2,8]: the electron effective mass in CaF_2 is $m_e = 1.0m_0$, the Si/CaF_2 conduction band offset is $\chi_e = 2.38$ eV) a detection of luminescence is used as the main method of electron transport diagnostics.

2. Samples fabrication

The investigation deals with the Au/CaF_2/p-Si(111) structures. The several monolayer (1 ML = 0.315 nm) CaF_2 films were fabricated by

* Corresponding author at: 26 Polytechnicheskaya, 194021 St. Petersburg, Russia. Tel.: +7 812 2976411.
E-mail address: ill-88@mail.ru (Yu.Yu. Illarionov).

0040-6090/$ – see front matter © 2013 Elsevier B.V. All rights reserved.
http://dx.doi.org/10.1016/j.tsf.2013.07.050

MBE on p-Si wafers with boron concentration $N_A = 10^{16}$ cm^{-3}. The lattice parameter of Calcium Fluoride (0.546 nm) is well-matched with that of Silicon (0.543 nm); the (111) orientation of Si substrate thermodynamically enables a growth of a homogeneous CaF_2 layer [2,9]. Application of the standard Shiraki method [10] for chemical treatment of Si substrate and MBE growth at an optimized temperature 250 °C allowed for obtaining high-quality pinhole-free films. Like in the most of works on CaF_2 MIS structures, gold was used for gate contacts (Au thickness 40 nm; diameter 80 μm). They were deposited on the top of fluorite layer through the special mask.

3. Concepts of MIS luminescence

In a MIS structure the electrons are injected from a metal gate into semiconductor under a positive substrate bias and should be highly energetic, i.e. "hot". Such electrons may be engaged into radiative transitions of different kind, like radiative recombination (RR) and intraband (IB) photon emission. In p-Silicon the luminescence phenomenon occurs under the accumulation condition, and the transitions take place at a mean free path distance (L ~ 10 nm) exceeding the band-bending region width (~2–3 nm) as shown in Fig. 1a. Whether the electrons are indeed hot depends on the transport mechanism. Assuming an elastic transport in CaF_2, the electrons will reach the mean free path distance with injection energy close to the metal Fermi level energy $E_{inj} = E_{Fm}$. Otherwise E_{inj} will be lower. In Fig. 1a, energy evolution in Si is schematized for two elastically transported electrons. It should be kept in mind that the optical transition can be preceded by multiple phonon scattering events, so that no sharp peaks are to be expected in the spectrum. In such a case, the photon energy ($\hbar\omega$) limits for IB radiation are 0 and $qV - q\Phi_F$, and for RR they are the silicon band-gap E_g and $qV - q\Phi_F + E_g$, with $q\Phi_F$ being the Si Fermi level respectively to the conduction band edge (depending on the doping N_A). The upper limit for RR accounts only for the holes near the valence band edge.

If light is detected within a narrow photon energy interval $\hbar\omega$… $\hbar\omega + \Delta\hbar\omega$ under the increasing bias voltage V, the activation thresholds of the intensity vs. voltage function $I^{\hbar\omega}(V)$ will be $qV_{RR} = \hbar\omega + q\Phi_F - E_g$ ($\hbar\omega > E_g$) for recombination and $qV_{IB} = \hbar\omega + q\Phi_F$ (any $\hbar\omega$) for IB radiation. The concepts of light emission from silicon-based MIS structures and a threshold picture were presented in more detail in [11]; so far emission was observed only in diodes with silicon dioxide films of different thickness [11–13]. From a formal viewpoint, the thresholds in the light-emission characteristics should appear for a MIS tunnel structure with an arbitrary dielectric. So, if some similar traditional materials like oxynitrides were employed instead of SiO_2, it could be questioned whether a repetition of luminescence studies [11,12] with another insulator deserves any attention. However a substitution to CaF_2 is a principal change, also taking in mind the present status of the fluoride growth technology. It is clear that the "correct" position of the above thresholds may be treated as a strong indicator for an elastic tunneling transport.

Noteworthy, all the earlier research on MIS structures with calcium fluoride was done with the samples grown on n-type Si [1–5] and Ge [14] substrates. However it is clear that such luminescence studies cannot be reasonably performed on n-type substrates because for such substrates a positive bias corresponds to an inversion-depletion regime. The optical transitions will therefore occur in the band bending region – and a straightforward interrelation between the threshold voltages and the selected photon energy will be impossible.

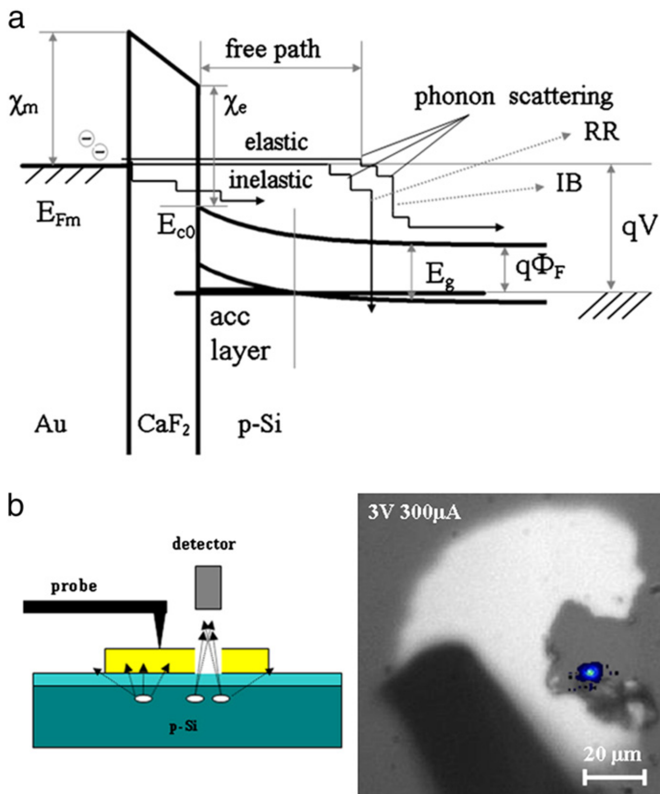

Fig. 1. (a) Band diagram of the Au/CaF_2/p-Si structure: origin of injection-related light emission. (b) *Left*: Experiment scheme; *Right*: Photon emission image overlaid on the reflection image. The emission spot is generated by an emission source closest to the edge of the contact. The probe is re-approached on the unscratched part of the electrode surface and thus the emission was detected from the scratched area.

4. Experimental technique

Optical characteristics of the fabricated samples were measured using a Photon Emission Microscopy system built at Singapore Institute of Manufacturing Technology (SIMTech) [15]. In addition to photon emission detectors the system has a camera observing the sample at a glazing angle. This camera allows more precise and softer landing of the tungsten probe on the soft electrode without mechanical damage. Two detectors were implemented: Pixis_1024 BR_Excelon was employed in a spectral range 500–900 nm and the detector Xenics Xeva-1200 was used within 900–1500 nm. The measurements were performed in a complete darkness to exclude any distortion of the photon emission signal. Originally, only weak emissions were observed along the electrode border. However, it was not clear whether the emission sources are crowded near the periphery or distributed underneath the entire electrode area. In order to check this issue the increased pressure on the tungsten probe was applied scratching away a portion of the gold contact. Similar partial removal of the contact had been performed on several electrodes and it was found that this process does not substantially affect the I-V characteristic of the device. At the same time it became clear that the light is emitted under the whole contact but is localized in the spots. In Fig. 1b an example is shown where the emission image is overlaid on top of the reflection image. The brightest emissions are generated in the small spot, indicating the locally confined current. However, it should be noted that this spot is brightest only because the opening in the electrode is very close to its location and there can be other bright spots hidden under the rest of the electrode. From practical viewpoint, a scratching procedure enabled the photon emission detection even at very low bias (~1.5 V, current J = 1–50 μA). Note that the positions of the emission spots are never changed during measurement. This is because a spatial distribution of the current and of the current-related radiation relies on the fluoride film topography; the spots being localized beneath the thinnest film regions.

5. Results and discussion

The measurements were performed within different spectral ranges. The intensity at a targeted wavelength (λ) was measured in arbitrary units as a difference of the detector counts obtained with two long-pass filters having close edge wavelengths λ_1, λ_2 surrounding λ. The photon energy is then evaluated as $\hbar\omega = 2\pi\hbar c/\lambda$ and the presence of luminescence thresholds is analyzed at different $\hbar\omega$ in Fig. 2, where all the intensities are normalized to a value of current J and plotted against the bias voltage V. The electrode-to-electrode reproducibility of the light-emission characteristics was quite satisfactory.

As one can see in Fig. 2 for most cases the thresholds are observed close to theoretical values. For example, the intensity vs. voltage curve measured with the 700 and 800 nm edged filters (on average, λ = 750 nm, i.e. $\hbar\omega = 1.65$ eV) exhibits $V_{RR} \approx 1.5$ V and $V_{IB} \approx 2.6$ V. Qualitatively the same features are present also for the λ = 550–650 and 900–1050 nm cases. However for a sub-E_g photon energy, there is no any RR contribution. So in the curve for a 1300–1400 nm wavelength range ($\hbar\omega = 0.92$ eV) only the IB threshold $V_{IB} \approx 1.85$ V can be found. Similar values can be obtained from the simple formulas $V_{RR} = \hbar\omega$ - $q\Phi_F$ and $V_{IB} = \hbar\omega$ - $q\Phi_F + E_g$ with $q\Phi_F \approx 0.95$ eV and $E_g \approx 1.12$ eV. This just says that a transport of electrons, at least in its substantial part, is an elastic transport. For the $\lambda = 600 \pm 50$ nm spectral range ($\hbar\omega = 2.07$ eV), the thresholds appear even earlier than indicated with dashed markers. It reveals a rawness of the "mean-λ treatment" with $|\lambda_1 - \lambda_2|$ ~ 100 nm for short wavelengths; the V_{RR} and V_{IB} positions agree better with the maximal Lambda (dotted markers). As to the dependence for $\hbar\omega = 1.27$ eV, it might be at any V somewhat affected by a contribution of RR transitions of thermalized electrons [11] as this $\hbar\omega$ is just a little higher than E_g; probably from this reason the curve looks generally more chaotic than the other three and its features are difficult to attribute.

Both RR and IB optical transitions can be classified down into the direct (vertical) and indirect ones. The former are generally known [16] to have higher probability. The threshold for a direct IB luminescence, $qV_{IB\text{-}d}$, is higher than qV_{IB} and can be calculated considering the full silicon band structure: $qV_{IB\text{-}d}(\hbar\omega) = E|_{E_{dir}(E)=\hbar\omega} + q\Phi_F$ (E_{dir} means the maximum direct-transition energy [11] among all states with the given energy $E = E_{inj} - E_{c\infty}$ where $E_{c\infty}$ is the bulk-Si conduction band edge). In some cases the IB-direct transitions were observed in our experiments on a background of indirect RR and IB radiation. Particularly, Fig. 2 exhibits $V_{IB\text{-}d} \approx 3.0$ V for $\hbar\omega = 1.65$ eV and $V_{IB\text{-}d} \approx 1.95$ V for $\hbar\omega = 0.92$ eV. These results are similar to the calculated values $V_{IB\text{-}d} \approx 2.94$ V ($\hbar\omega = 1.65$ eV) and $V_{IB\text{-}d} \approx 1.92$ V ($\hbar\omega = 0.92$ eV). For the photon energy $\hbar\omega = 2.07$ eV, like it was with RR and an indirect IB light emission, the IB-d threshold is lower than its prediction $V_{IB\text{-}d} = 3.53$ V, owing to a too wide range $\lambda_1 \ldots \lambda_2$.

Because of a lack of signal intensity, the thresholds could not always be discerned in the $I^{\hbar\omega}(V)$ curves. The same reason enforced large spectral intervals; qualitatively identical results were obtained with the pairs of filters having smaller edge wavelength difference but suffered from noise problems. Nevertheless it can anyway be claimed that some hot-electron-injection-induced luminescence is observed for every Au/CaF_2/pSi structure.

Unless the bias exceeded 3.0–3.5 V, the intensity–voltage curves of Fig. 2 can be re-recorded almost exactly. However, after overloading the sample radiation always becomes much weaker although is still not fully quenched. The thresholds are being shifted toward higher applied voltages and broadened (see inset $\hbar\omega = 1.65$ eV in Fig. 2c, logarithmic scale). This indicates the appearance of the energy losses during an electron transport through the damaged fluoride film. Usually, even after damage, the spot positions remain stable, but the lateral spot sizes shrink. Anyway, in order to evade any degradation

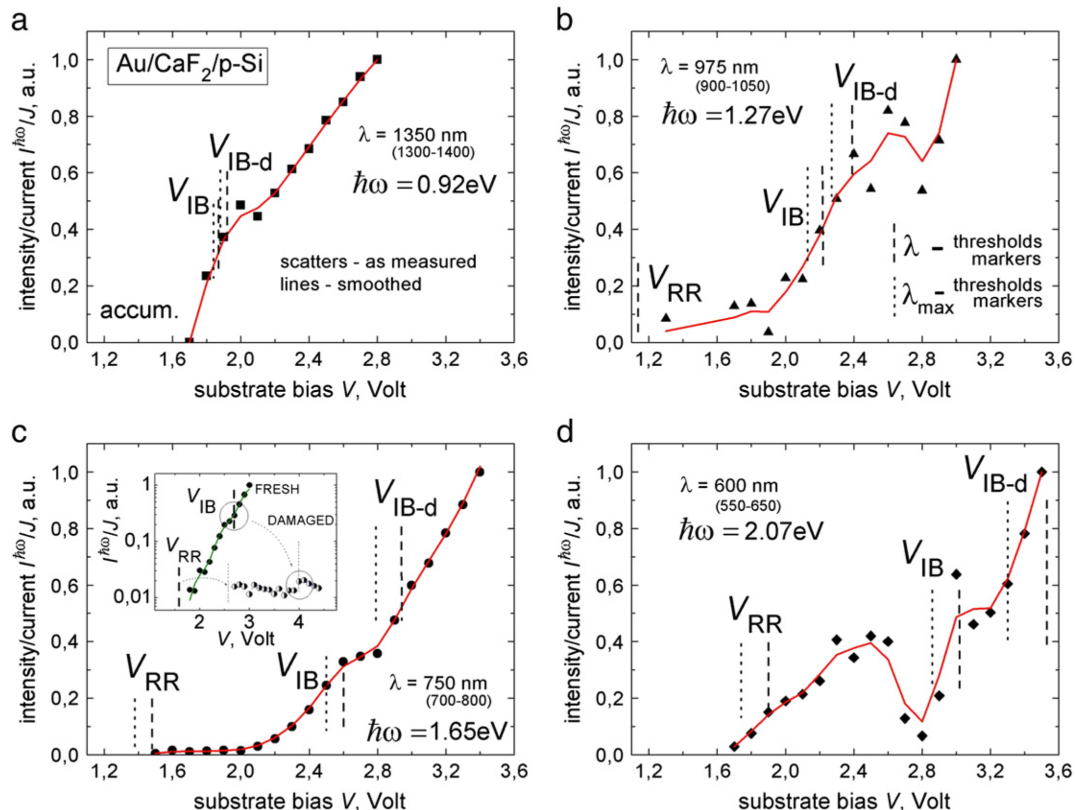

Fig. 2. Voltage dependence of the intensity of photon emission from the Au/CaF_2/p-Si(111) structures. Each curve is normalized by its maximum value.

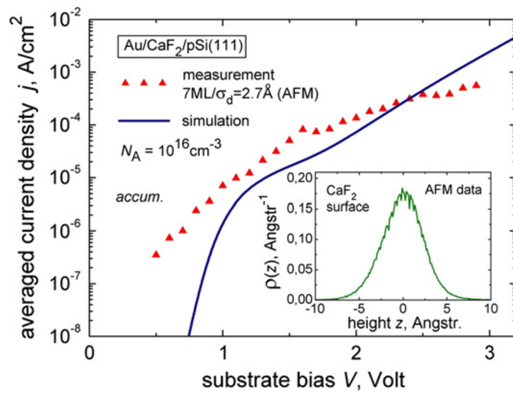

Fig. 3. Measured current–voltage curve ("+" to Si) of Au/CaF_2/p-Si(111) structure reproduced with the simulation model considering thickness fluctuation.

issues, the measurements for each part (a-d) of Fig. 2 have been performed with an individual virgin electrode.

The observation of optical characteristics allows for solidifying the more casual "electrical" data presented in Fig. 3 which alone might look less convincing. One may claim there is a satisfactory agreement between the experimental curve and the simulations performed assuming the fluoride thickness fluctuation $\sigma_d = 0.27$ nm, normal-weighted. This value is not taken as a fitting parameter but extracted from the AFM (atomic-force-microscopy) images recorded for the same sample (inset). For a tunnel-thin film this sigma value is rather large considering a very strong dependency of a current density on the local thickness. This reveals technological imperfections. Optical behavior, however, confirms that, despite these deficiencies, the transport mechanism remains as elastic tunneling. This means that crystalline quality and injection capability of the grown fluoride layers are rather good. (The simulation technique applied to generate the curves in Fig. 3 relied on the regular models of a MIS tunnel structure amended in such a way that to account for a large transverse momentum of the tunneling electrons. Namely, the tunnel probability T was calculated [17] depending on the energy E and on the transverse momentum $k_\perp$ without substituting $k_\perp$ through a so-called transverse energy $E_\perp$. The Au/CaF_2 barrier is $\chi_m = 2.63$ eV.) Note that a theory-to-experiment agreement in Fig. 3 could be artificially improved by a slight modification of the barrier parameters. However it is more striking that a reasonable – maybe not ideal – coincidence is possible even without any adjustments. The opposite-polarity branch ("−" to Si) is not shown and not relevant for this work as there occurs no light emission under that condition. Moreover the current flow for $V < 0$ is regulated not only by the tunnel barrier, but also (and to a large extent) by a minority carrier generation in the substrate [7], which complicates any interpretations.

6. Conclusions

To summarize, using luminescence measurements we confirmed the elastic tunneling transport in thin calcium fluoride layer. This observation is important for application of the MIS structures with CaF_2 as a hot electron injector. Especially valuable is this result in context of the resonant tunneling diodes. To some extent this is also not unimportant for other applications, such as gate insulator in the field effect transistors. A possibility of fabrication of MIS structures with calcium fluoride showing the luminescence thresholds is by far not a trivial technological result.

On the other hand, the revelation of light emission from the Au/CaF_2/pSi capacitor is interesting as an additional manifestation – in the structure with a very different insulator than SiO_2 – of the light emission capability of a MIS tunnel diode in general. As a further development of this research it would be interesting to perform the measurements of complete spectra. This will allow for estimating the fraction of elastic component in a total current from the comparison between the recorded and theoretical spectra.

Acknowledgements

The authors are grateful to Dr. D.V. Isakov, Dr. B.P. Ng and Dr. S.W. Kok (SIMTech) for their collaboration and to European Commission (Erasmus Mundus and ONDA project FP7-PEOPLE-2009-IRSES-247518) for the financial support.

References

[1] C. Deiter, M. Bierkandt, A. Klust, C. Kumpf, Y. Su, O. Bunk, R. Feidenhans'l, J. Wollschläger, Phys. Rev. B. 82 (2010) 085449.
[2] M.I. Vexler, N.S. Sokolov, S.M. Suturin, A.G. Banshchikov, S.E. Tyaginov, T. Grasser, J. Appl. Phys. 105 (2009) 083716.
[3] M. Watanabe, Y. Iketani, M. Asada, Jpn. J. Appl. Phys. 39 (2000) L964.
[4] M. Watanabe, T. Funayama, T. Teraji, N. Sakamaki, Jpn. J. Appl. Phys. 39 (2000) L716.
[5] K. Sadakuni-Makabe, M. Suzuno, K. Harada, H. Akinaga, T. Suemasu, Jpn. J. Appl. Phys. 49 (2010) 060212.
[6] M.I. Vexler, N. Asli, A.F. Shulekin, B. Meinerzhagen, P. Seegebrecht, Microelect. Eng. 59 (2001) 161.
[7] A. Schenk, Advanced physical models for Silicon device simulations, Springer, Wien, NY, 1998. , (Chapt. 5.).
[8] In: W. Hayes (Ed.), Crystals with the Fluorite Structure: Electronic, Vibrational, and Defect Properties, Clarendon Press, Oxford, 1974.
[9] L.J. Schowalter, R.W. Fathauer, Crit. Rev. Solid State Mater. Sci. 15 (1989) 367.
[10] A. Ishizaka, Y. Shiraki, J. Electrochem. Soc. 133 (1986) 666.
[11] N. Asli, M.I. Vexler, A.F. Shulekin, P.D. Yoder, I.V. Grekhov, P. Seegebrecht, Microelectron. Reliab. 41 (2001) 1071.
[12] E. Cartier, J.C. Tsang, M.V. Fischetti, D.A. Buchanan, Microelect. Eng. 36 (1997) 103.
[13] G. Deboy, J. Kölzer, Semicond. Sci. Technol. 9 (1993) 1017.
[14] T. Oshita, K. Takahashi, K. Tsutsui, J. Cryst. Growth 31 (2009) 2224.
[15] B.P. Ng, Y. Zhang, S.W. Kok, Y.C. Soh, Ultramicroscopy 109 (2009) 291.
[16] J. Bude, N. Sano, A. Yoshii, Phys. Rev. B. 45 (1992) 5848.
[17] M.I. Vexler, M.I. Vexler, Yu.Yu. Illarionov, S.M. Suturin, V.V. Fedorov, N.S. Sokolov, Phys. Solid State 52 (2010) 2357, (translated from Russian).